Transport and speciation of uranium in groundwater-surface water systems impacted by legacy milling operations

Patrick Byrne[1,], Christopher C. Fuller[2], David L. Naftz[3], Robert L. Runkel[4], Niklas J. Lehto[5], William L. Dam[6]*

[1]School of Biological and Environmental Sciences, Liverpool John Moores University, Liverpool, L3 3AF, United Kingdom

[2]U.S. Geological Survey, 345 Middlefield Road, Menlo Park, CA 94025, U.S.A.

[3]U.S. Geological Survey, 3162 Bozeman, Helena, MT 59601, U.S.A.

[4]U.S. Geological Survey, 3215 Marine St, Boulder, CO 80303, U.S.A.

[5]Faculty of Agriculture and Life Sciences, Lincoln University, Lincoln 7647, New Zealand

[6]Conserve-Prosper LLC, Grand Junction, Colorado 81507, U.S.A.

*Corresponding author. Email: p.a.byrne@ljmu.ac.uk; Tel: +44-(0)115-231-2297

Submitted to: Science of the Total Environment

Date of submission: 27th July 2020

Keywords: uranium; groundwater; surface water; speciation; DGT; DET

ABSTRACT

Growing worldwide concern over uranium contamination of groundwater resources has placed an emphasis on understanding uranium transport dynamics and potential toxicity in groundwater-surface water systems. In this study, we utilized novel in-situ sampling methods to establish the location and magnitude of contaminated groundwater entry into a receiving surface water environment, and to investigate the speciation and potential bioavailability of uranium in groundwater and surface water. Streambed temperature mapping successfully identified the location of groundwater entry to the Little Wind River, downgradient from the former Riverton uranium mill site, Wyoming, USA. Diffusive equilibrium in thin-film (DET) samplers further constrained the groundwater plume and established sediment pore water solute concentrations and patterns. In this system, evidence is presented for attenuation of uranium-rich groundwater in the shallow sediments where surface water and groundwater interaction occurs. Surface water grab and DET sampling successfully detected an increase in river uranium concentrations where the groundwater plume enters the Little Wind River; however, concentrations remained below environmental guideline levels. Uranium speciation was investigated using diffusive gradients in thin-film (DGT) samplers and geochemical speciation modelling. Together, these investigations indicate uranium may have limited bioavailability to organisms in the Little Wind River and, possibly, in other similar sites in the western U.S.A. This could be due to ion competition effects or the presence of non- or partially labile uranium complexes. Development of methods to establish the location of contaminated (uranium) groundwater entry to surface water environments, and the potential effects on ecosystems, is crucial to develop both site-specific and general conceptual models of uranium behavior and potential toxicity in affected ground and surface water environments.

1. Introduction

Uranium (U) is a radioactive element with a crustal concentration of approximately 2.7 mg kg^{-1} (Gupta and Singh, 2003), and is found with concentrations of 12 ng L^{-1} to 4.8 µg L^{-1} in stream water worldwide (Windom et al., 2000) and approximately 3.4 µg L^{-1} in sea water (Dunk et al., 2002). It occurs in the environment as a result of natural weathering of U-rich sediments and rocks or via anthropogenic activities such as mining, nuclear accidents and waste disposal, as well as nuclear weapons testing and disposal (Abdelouas, 2006; Guo et al., 2016; Nolan and Weber, 2015). In aqueous environments, U exists primarily in the hexavalent oxidation state (U(VI)) as the uranyl ion (UO_2^{2+}) at pH <5, or as stable uranyl hydroxide or carbonate complexes (e.g. $UO_2(CO_3)_2^{2-}$) at pH >7 (Nolan and Weber, 2015). The tetravalent state (U(IV)) is much less soluble and known to accumulate in anoxic sediments such as ore deposits and contaminated aquifers (Bone et al., 2017a; Bone et al., 2017b).

As a non-essential trace metal and radionuclide, U can be highly toxic due to both its chemical (speciation) and radiological (isotopic composition) properties, and exposure to U through drinking water is associated with nephrotoxic effects (Bjørklund et al., 2020; Pinney et al., 2003). As a consequence, the U.S. Environmental Protection Agency and the World Health Organization have set environmental guideline levels of 30 µg L^{-1} in drinking water (U.S. Environmental Protection Agency, 2000; World Health Organization (WHO), 2012). In recent years, U has emerged as a widespread threat to human health and ecosystems due to elevated concentrations in groundwater from historical uranium mining and processing, nuclear waste disposal, and natural geogenic sources (Bone et al., 2017b; Coyte et al., 2018; Nolan and Weber, 2015). Furthermore, the growing worldwide demand for groundwater as a source of water (Dalin et al., 2017), and for

66 U as a source of energy (World Nuclear Association, 2019), has raised concerns regarding the
67 future risks to humans and ecosystems of U-contaminated groundwater.

68 Uranium is one of the principal contaminants at former mill sites managed by the U.S.
69 Department of Energy's (DOE) Office of Legacy Management (Dam et al., 2015). Typically, U
70 ore was crushed and ground into small particles in the milling process before being leached to
71 dissolve U oxides into a concentrated liquid slurry. Decades of U ore processing for use in the U.S.
72 Government nuclear weapons and energy programs resulted in the accumulation of approximately
73 30 Mm^3 of U ore processing waste (U.S. Department of Energy, 2020). Tailings that remained
74 after the milling process were generally held in unlined impoundments resulting in widespread
75 groundwater contamination in the western U.S.A. (U.S. GAO (U.S. Government Accountability
76 Office), 2020). Today, the environmental liability of the DOE is estimated at USD$7.35 billion,
77 with approximately 40% of these costs associated with long-term monitoring and maintenance
78 (U.S. GAO (U.S. Government Accountability Office), 2020). Contamination of groundwater used
79 for drinking and irrigation water is a major concern (U.S. GAO (U.S. Government Accountability
80 Office), 2020). However, the interaction of U-rich groundwater with surface water systems and
81 the potential effects on freshwater ecosystems has not previously been considered. Yet, the ability
82 to locate groundwater plumes, to establish the effect on receiving surface water systems, and to
83 establish the potential bioavailability of U to freshwater ecosystems, are seen as key requirements
84 to meet the long-term monitoring and remediation objectives set out by the DOE (U.S. GAO (U.S.
85 Government Accountability Office), 2020).

86 Recognizing the challenges associated with monitoring the potential human and ecological
87 effects of U-contaminated groundwater, the DOE, in collaboration with the U.S. Geological
88 Survey, University of Montana, Liverpool John Moores University, and Northern Arapahoe Tribe,

89 conducted a pilot-scale investigation of groundwater-surface water interaction at the former U ore
90 mill and processing site at Riverton, Wyoming, from 2015 to 2018. The overall aim of this research
91 was to test and apply a range of hydrological, geophysical, ecological and biogeochemical tools
92 and methods to identify and quantify the effect of groundwater U plumes on connected surface
93 water environments. As such, the research presented in this contribution is part of a larger and
94 ongoing interdisciplinary study – project data is available in Naftz et al. (2019) and Terry and
95 Briggs (2019).

96 In this specific study, we present a novel approach to establish the water quality and potential
97 biological effects of contaminated (U) groundwater interaction with surface waters. The approach
98 utilizes streambed temperature mapping as an inexpensive and unobtrusive method for identifying
99 groundwater fluxes through the streambed at small spatial scales (Conant, 2004). Areas of
100 groundwater efflux are then targeted using diffusive equilibrium in thin-film (DET) samplers to
101 establish spatial and vertical patterns of U sediment pore water chemistry. Diffusive gradients in
102 thin-film (DGT) samplers, in conjunction with speciation modelling, are then used to investigate
103 the potential bioavailability of U in ground and surface waters. Both DET and DGT samplers have
104 previously been used to establish U concentrations and speciation in surface waters (Drozdzak et
105 al., 2016; Hutchins et al., 2012; Turner et al., 2014; Turner et al., 2012) and in sediments in
106 laboratory microcosm experiments (Gregusova and Docekal, 2013). However, our study is the first
107 to apply DET and DGT techniques in-situ to investigate U concentrations, transport and speciation
108 in a groundwater-surface water system. This represents a substantial contribution to our conceptual
109 understanding of U behavior and potential toxicity in affected ground and surface water
110 environments.

Our primary aim was to demonstrate the potential of using in-situ temperature, DET and DGT samplers, in conjunction with speciation modelling, to establish the effect of legacy U groundwater plumes on connected surface waters. The specific objectives were to: (1) establish the location, magnitude, and effect of contaminated groundwater efflux to surface water, and; (2) establish the speciation and potential bioavailability of U at the groundwater-surface water interface and in surface water systems.

2. Methodological approach

2.1 Study area

The Uranium Mill Tailings Radiation Control Act (UMTRCA) was enacted in the U.S.A. in 1978 to provide for the safe disposal and long-term stabilization of U mill tailings to minimize environmental and human health risks (U.S. Department of Energy, 2020). Twenty-two mill sites were effectively abandoned when UMTRCA was passed; these were designated as Title I sites where DOE has responsibility for long-term monitoring and remediation, including removal of residual surface wastes. Title II sites (six sites) continued to operate, or commenced processing activities, after UMTRCA was passed, and responsibility for their remediation falls to the licensee.

The Riverton site is situated on an alluvial terrace in the Wind River Basin, Wyoming, U.S.A. Groundwater flow direction is generally southeast and occurs in three aquifers beneath the site (U.S. Department of Energy, 1998): (1) a shallow, unconfined aquifer, consisting of approximately 4.6 – 6 m of unconsolidated alluvial material, and underlain by a discontinuous shale confining layer 2 – 3 m thick; (2) a middle, semi-confined aquifer; and (3) a deeper, confined aquifer comprising the upper units of the Eocene Wind River Formation. The climate of the region is semi-arid to arid, with mean annual precipitation approximately 20 cm (the majority occurring April –

June as spring snows and showers) (U.S. Department of Energy, 1998). Phreatophytes cause evapotranspiration to vary daily and seasonally in response to seasonal climate and plant growth factors (Dam et al., 2015).

The Riverton Processing site (Title I) produced yellowcake (U_3O_8), used in the preparation of U fuel for nuclear reactors and weapons, from 1958 to 1963 and was located on the Wind River Indian Reservation near Riverton, Wyoming (Figure 1). The mill processed a total of 816,470 tonnes of U ore that was mined in the Gas Hills mining district in Wyoming (Merritt, 1971). During the milling process, ore was crushed and ground, and water was added to create a slurry. Mill tailings that remained after extraction of U were conveyed by slurry to a 29 hectare unlined tailings impoundment and stockpiled (U.S. Department of Energy, 1995). Following the UMTRCA, surface remediation of the site was completed by DOE in November 1989. Approximately, 1.4 Mm^3 of contaminated material was removed from the site; however, decades of leaching of the tailings slurry has led to contamination of the shallow groundwater beneath and downgradient from the site. The primary contaminant is U, but other trace elements (arsenic (As), boron (B), iron (Fe), lead (Pb), manganese (Mn), mercury (Hg), molybdenum (Mo), nickel (Ni), selenium (Se), vanadium (V)), and sulfate (SO_4) are above background concentrations (Narasimhan et al., 1986; U.S. Department of Energy, 1998; White et al., 1984).

The approach taken by DOE to the management of groundwater contamination at Riverton and other UMTRCA sites was based on the natural flushing compliance strategy, where modelling of contaminant movement in aquifers using the Groundwater Analysis and Network Design Tool (GANDT) predicted U concentrations falling below the maximum contamination level (30 $\mu g\ L^{-1}$) within a 100 year regulatory timeframe (Dam et al., 2015). Prior to 2010, groundwater monitoring indicated that U concentrations at the Riverton Processing site were decreasing at a

steady rate and were in general agreement with the GANDT modelling predictions (Dam et al., 2015; U.S. Department of Energy, 2009). However, a series of flood events beginning in June 2010 mobilized contaminants held in normally unsaturated materials above the alluvial water table, as well as contaminants within the aquifer (Dam et al., 2015; Ranalli and Naftz, 2014), resulting in substantial increases in groundwater U concentrations in some monitoring wells and possible increased flux of contaminants to the Little Wind River. Groundwater monitoring data from other U ore processing sites reveals similar diversions from conceptual models of U attenuation over time (Shafer et al., 2014; Zachara et al., 2013). Further research on the interaction of legacy groundwater plumes with surface waters is therefore needed to help refine natural flushing predictions.

2.2 Streambed temperature mapping

A streambed temperature survey (following Conant, 2004) was conducted in August 2017 using a Traceable Control Company digital thermometer with a 10 cm probe. Measurement locations were surveyed with sub-meter accuracy using a Trimble R1 GNSS Receiver. Streambed temperature mapping areas were constrained to potential areas where the legacy groundwater plume intersected the left bank of the Little Wind River. Mapped areas were further constrained by stream channel material that would allow full penetration of the temperature probe. Transition from sand / silt to cobble bottom material prevented the extension of temperature maps beyond ~ 10 to 25 m from the left bank of the study reach. Areas where groundwater appeared to be closest to the sediment-water interface were selected for deployment of sediment DET and DGT probes.

2.3 DET and DGT probes: sediment and surface water deployments

Diffusive gradients in thin-films (DGT) and diffusive equilibrium in thin-films (DET) are methods of measuring fine-scale (cm to mm) solute concentrations in surface waters and sediment pore waters (Davison and Zhang, 2016). They have been used to quantify contaminant concentrations and biogeochemical processes in a variety of environments, including lacustrine (Ma et al., 2020; Zhang et al., 1995), estuarine (Cánovas et al., 2020), marine (Parker et al., 2017), and freshwater sediments (Byrne et al., 2015). Typically, DET devices are used to measure equilibrium surface water and sediment pore water concentrations by allowing solutes to diffuse through a membrane layer (0.45 μm) into an inner hydrogel layer (usually 0.12 cm thick). The time to reach equilibrium depends on the thickness of the DET material diffusion layer (combined hydrogel and membrane layer thickness), the difference between concentrations inside and outside the diffusion layer, and the rate of diffusion. Under the deployment conditions of this study (U diffusion coefficient: 3.11×10^{-6} cm^2 s^{-1} for sediment pore waters and 4.44 x 10^{-6} cm^2 s^{-1} for stream water based on different pH; Hutchins et al. (2012)), the U concentration in a freshly deployed DET probe is expected to have reached 95% of the surrounding water concentration at 124 min.

After deployment, the solute in the hydrogel can be sliced into segments (usually 0.2 to 1 cm) that can be eluted and analyzed for solutes of interest. The major advantage of the technique over other in-situ methods of sediment pore water sampling (e.g. drive points, dialysis peepers) is that measurements can be made at a higher spatial (vertical) resolution, although the sampling depth is typically restricted to 15 cm by the geometry of the commercially available probe housing (DGT Research Ltd., www.dgtresearch.com). In addition, DET probes typically sample a very small volume of sediment pore water (1 cm depth intervals = 0.1 cm x 1 cm x 1.8 cm = ~ 0.18 cm^3) perpendicular to the probe interface. This means there is very little disturbance or averaging of

pore water concentrations and chemical gradients, compared to other pore water sampling methods (Stockdale et al., 2009).

The DGT technique measures the diffusive flux of solute from sediment pore water by introducing a localized sink for the solute in the form of an ion-binding layer that is separated from the sediment pore water by a well-defined material diffusion layer consisting of a filter and hydrogel. Following deployment, a linear diffusion gradient is rapidly (< 60 min) formed across the diffusion layer and solute progressively accumulates in the binding layer (Davison and Zhang, 2016). The binding layer can then be analyzed to show spatial differences in the solute fluxes across the probe interface. As the DGT measures the flux of solute into the resin at a given location, it can provide highly localized information about solute mobilization / sequestration processes over the deployment period (Lehto, 2016). Moreover, because the resin layer mostly binds free ions and ions that can be released by labile or partially labile complexes, it can provide unique information about the speciation and bioavailability of solutes in-situ (Amato et al., 2014; Davison and Zhang, 2012; Zhang et al., 1995).

For groundwater (shallow sediment) deployments, a network of 10 DGT and 10 DET probes were deployed in pairs (within approximately 30 cm of each other) in August 2017 in the sediment on the left bank of the study reach along the Little Wind River (Figure 1). The sediment probes were 15 cm in length and deployed vertically in the sediment. It is worth noting that deployment of DET and DGT sediment probes is typically constrained to sand-dominated sediments that allow easy insertion of the plastic device into the sediment. However, stainless steel holders have been used to successfully deploy DET probes in coarse riverbed environments (Ullah et al., 2012). The probes were retrieved after 48 hours (DET) and 72 hours (DGT) and processed (see section 2.4) within 2 hours of retrieval at the U.S. Geological Survey laboratory in Riverton, Wyoming. The

hydrogel layers in the DET and DGT devices were 0.118 cm and 0.078 cm thick, respectively, and used a 0.014 cm thick polyethersulfone membrane (0.45 μm pore size) to separate the hydrogel from the sediment. Numerical modelling of the lateral diffusion of U (using DIFS: (Harper et al., 2000)) within the material diffusion layer found that the mean gel concentrations at distances of 1 cm and 2 cm intervals were 60% and 13% of the pore water concentrations at the origin after 48 h, respectively. For surface water deployments, DET and DGT 'piston' samplers were situated at three locations on the left bank of the Little Wind River: (1) 500 m upstream and (2) 450 m downstream from the cold water anomaly indicated by streambed temperature mapping, and (3) approximately 100 m downstream from the cold water anomaly and suspected groundwater efflux zone (Figure 1). At surface water sampling sites, DET and DGT probes were deployed in triplicate and retrieved and processed as per the shallow sediment deployments. Surface water 'grab' samples were also collected along river transects that overlapped the location of DET and DGT surface water probes. In this instance, samples were collected from the left, center and right side of each transect. Samples were filtered (0.45 μm) on-site and preserved with 1M HNO_3 to await analysis. Further information on the surface water grab sampling procedure are provided in the supplementary information.

The binding layer utilized in DGT devices used a Metsorb^{TM} (TiO_2) sorbent, which has been shown to be suitable for U measurements in freshwaters (Turner et al., 2014; Turner et al., 2012). All DET and DGT probes were supplied by DGT Research Ltd. (Lancaster, UK).

2.4 Laboratory and analytical procedures

In the laboratory, the sediment DGT and DET probes were sliced into 1 cm sections. The hydrogel and binding layers were removed from the DET and DGT probes, respectively, and

248 eluted for 24 hours in 10 mL 1M HNO_3 to await analysis. The solutions (including surface water
249 grab samples) were then analyzed by ICP-MS for target analytes (U and strontium (Sr)). Analysis
250 by ICP-MS utilized rhodium as an internal standard to compensate for analytical drift. Instrument
251 detection limits (IDL = 3.3σ / s) were 0.004 μg L^{-1} and 0.8 μg L^{-1} for U and Sr, respectively. High
252 precision and accuracy of the control standards (±4%) and certified reference material (SLRS-6)
253 (±7%) was achieved. The DGT results are expressed as solute concentrations (C_{DGT}) to help
254 comparison with the DET results. The standard equations used to calculate C_{DGT} are given in the
255 supplementary information.
256
257 *2.5 Validation of DGT probes*
258 Accumulation of solutes in the DGT device is known to be limited by the buffering capacity
259 of the sediment or water environment. If the flux [ng cm^{-2}] demanded by the DGT is in excess of
260 solute re-supply, then C_{DGT} may be substantially lower than solute concentrations derived from
261 DET measurements. To test the relation between the flux demanded by the DGT and the actual
262 flux from surface water and sediment pore waters, five sets of DGT 'piston'-style probes (Model:
263 R-SLU, DGT Research Ltd.) with different material diffusion layer thicknesses (filter and
264 hydrogel: 0.054, 0.092, 0.132, 0.170 and 0.208 cm) were inserted into the sediment (10 cm depth)
265 and suspended in the river water at site WR17-6 for 72 hours (Figure 1), each set consisted of three
266 replicate probes. If the flux from surface water and sediment pore waters meets or exceeds the
267 DGT demand over the length of the deployment, a plot of measured mass per unit area versus the
268 material diffusion layer thicknesses should be linear (Zhang et al., 1995).
269
270 *2.6 Geochemical speciation modelling*

Dissolved U(VI) speciation was calculated using PHREEQC (Parkhurst and Appelo, 2013) for sediment pore waters using the major ion chemistry for minipiezometer samples collected at 15 cm depth within 1 m of each DET / DGT deployment site and for surface water using averaged major ion chemistry along the study reach (which varied less than 3% among nine surface water grab sample sites) (data available in Naftz et al., 2019). PHREEQC calculations were conducted at 25 °C using the wateq4 database and included aqueous U species stability constants from Guillaumont et al. (2003). Because of their importance on U speciation and solubility, stability constants for ternary (Ca,Mg)-U(VI)-CO_3 complexes were included (Dong and Brooks, 2006; Dong and Brooks, 2008). Thermodynamic data for adjusting many of the U stability constants to the experimental temperature are not available. Oxic conditions were imposed in the PHREEQC speciation calculations because measured dissolved oxygen levels at 30 cm depth were equal to or greater than 0.4 mg L^{-1} (Naftz et al, 2019). Dissolved oxygen was not measured at shallower depths, with surface water dissolved oxygen. Dissolved uranium is thus assumed to be all in +6 oxidation state, (U(VI)). Dissolved Fe and Mn were not included in speciation calculations.

3. Results and Discussion

3.1 Transport of uranium from groundwater to surface water

Contour maps of streambed temperatures were constructed for the sampling period in 2017 (Figure 2a). The < 25th percentile of streambed temperature was identified to provide a point of reference to denote areas with a higher potential for groundwater discharge through the streambed. The colder areas of streambed sediment were limited to narrow (< 5 m) areas along the left bank of the active channel to the north of the study area (Figure 2a). Streambed temperature values in

293 the southwest corner of the study area were generally > 25th percentile of the streambed
294 temperature values except for one small area (sample point WR17-1) (Figure 2a).

295 Identification of the groundwater efflux (cold water anomalies) from the streambed
296 temperature survey (Figure 2a) guided the selection of sediment pore water DET and DGT
297 sampling sites. Contour maps of DET U concentrations in the sediment pore waters (top 15 cm)
298 along the Little Wind River study reach during August 2017 are presented in Figure 2b, and
299 concentration statistics are summarized in Table 1. Site WR17-1 (upgradient from the groundwater
300 plume) and site WR17-10 (downgradient from below the groundwater plume) are not shown as
301 mean sediment pore water concentrations of U were low (WR17-1, 22 µg L^{-1}; WR17-10, 11 µg L^{-1}
302), and these sites appeared not to be influenced by contaminated groundwater. The DET probes
303 clearly identified the location and focus of contaminated groundwater in the shallow sediments of
304 the Little Wind River. The shallow portions of the plume appeared to be constrained to an
305 approximately 140 m distance along the channel, its approximate boundaries aligning with sites
306 WR17-9 (upstream) and WR17-8 (downstream). The mean background U concentration (from site
307 WR17-1) was 22 µg L^{-1}. However, the mean U concentration within the groundwater plume zone
308 was 570 µg L^{-1} (range = 30 to 1321 µg L^{-1}), with the peak concentrations centered on site WR17-
309 6. Direct comparison of these shallow sediment pore water concentrations with other sites is not
310 possible; however, comparison with groundwater samples from Riverton (1 m depth) (Naftz et al.,
311 2019) and other UMTRCA sites (> 1 m depth) (Green River, L-Bar, Naturita, Shiprock, and Tuba
312 City, Figure 1) (U.S. Department of Energy Legacy Management, 2020) indicates the DET U
313 concentrations are within the general range reported (13 µg L^{-1} to 7100 µg L^{-1}).

314 Between sites WR17-4 and WR17-7, U concentrations decreased towards the surface above
315 approximately 6 to 7 cm depth (allowing for uncertainty arising from lateral diffusion in the probe),

316 potentially limiting surface water contamination. Decreases in sediment pore water solutes in near-
317 surface riverbed sediments has been linked to either physical dilution with infiltrating and lower
318 concentration surface water (Byrne et al., 2014), or sorption or precipitation of mineral phases
319 along a biogeochemical gradient (Fuller and Harvey, 2000). To investigate the process driving
320 attenuation of U in the shallow sediments, we consider Sr concentrations here as an indicator of
321 the degree of groundwater-surface mixing. Strontium is generally considered to behave
322 conservatively in groundwater-surface water systems, and so any decrease in concentration in the
323 sediment pore waters are likely related to mixing with surface waters that would contain lower Sr
324 concentrations (Petelet-Giraud et al., 2018). Figure 2c illustrates a contour map of Sr pore water
325 concentrations from the DET samplers. Unlike U concentrations, elevated Sr pore water
326 concentrations at sites WR17-5, -6 and -7 (range: 4.6 to 7.4 mg L^{-1}) persisted closer to the surface
327 (surface water = 1.1 mg L^{-1}), with some evidence for decreases at site WR17-7 (to 2.8 mg L^{-1}). .
328 These slightly different patterns in reactive and conservative solute concentrations indicate both
329 dilution by infiltrating low U concentration surface water (Table 1) and reactive uptake of U in
330 groundwater by sediments during hyporheic mixing may account for the observed decrease in U
331 concentrations. However, the specific geochemical and hydrological processes driving the
332 observed solute concentrations and patterns are not resolved in this study but are currently being
333 investigated.

334 The effect of the groundwater plume on U concentrations in the Little Wind River is illustrated
335 in Figure 3. Both surface water grab and DET samples showed a longitudinal increase in U
336 concentrations from upstream from the plume to the approximate central location of the plume
337 (Figure 3a and 3b). Mean grab sample U concentrations were lower than the U-DET concentrations
338 and also indicated an increase of U concentrations downstream from the plume area where the

DET samples showed a decrease. In this instance, the DET samplers were located closer (within 1 m) to the left bank of the Little Wind River than the grab samples and so probably represent higher concentration and poorly mixed plume-derived waters 'hugging' the left bank of the river. As the grab samples were collected from different locations across river transects, the mean of these values incorporates the effect of mixing and is therefore a better representation of longitudinal changes in U concentrations in this relatively wide river channel. Although DET samples were not taken in the same manner as grab samples on this occasion, the DET data still demonstrate a change in surface water U concentrations associated with contaminated groundwater efflux to the river. A longitudinal increase in surface water U concentrations from upstream to downstream from the plume area was also demonstrated in 2016 under lower river flow conditions (see supplementary information and Figure S1) and, as far as the authors are aware, this is the first time that groundwater with elevated U has been shown to increase river water U concentrations at UMTRCA sites. This is despite regular and long-term monitoring of surface waters by DOE and may indicate that the DOE sampling strategy at UMTRCA sites is not representative of locations of contaminated groundwater discharge.

3.2 Exploring uranium speciation in sediment pore waters and surface water

Sediment pore water and surface water C_{DGT} U concentrations were substantially lower than concentrations derived from DET measurements (Table 1); the mean C_{DGT} for U across all ten sample sites was 15 μg L^{-1} (range: 1 to 122 μg L^{-1}). It is not uncommon for sediment pore water and surface water concentrations derived from DET, drive point samplers, or grab samples to be higher than C_{DGT} (Davison and Zhang, 2012). Typically, there are three possible causes for this. First, re-supply of solute from sediment pore water to the DGT may not be sufficient to meet the

demand from the DGT (Lehto, 2016). Second, the binding gel may not be able to remove the target solute from solution rapidly due to competition for binding sites with other solutes (Bennett et al., 2016). Third, the solute of interest may not exist in available forms and are instead partially labile or inert to DGT; this has been used to imply potential constraints to solute bioavailability (i.e. solute that could potentially be absorbed and retained by an organism) (DeGryse and Smolders, 2016). Complexes with large dissolved organic ligands often have small diffusion coefficients and can be less labile than dissolved inorganic complexes (Davison and Zhang, 2012).

We can investigate the possibility of solute demand from the DGT exceeding solute supply from the sediment pore waters by calculating $R_{c,72hr}$, the ratio of C_{DGT} from a 72 hour deployment to the bulk pore water concentrations (from DET measurements) (Figure 4) (Lehto, 2016). Numerical modelling carried out with the DGT-induced fluxes in sediments model (Harper et al., 1998; Menezes-Blackburn et al., 2019) (assuming sediment porosity of 0.8), indicates that values of $R_{c,72hr}$ greater than 0.80 would indicate a well-buffered system with continuous supply from the solid- and solution phases at a rate almost equal to the flux demanded by the DGT, while values approaching 0.07 would indicate an increasingly diffusion-driven supply. In this scenario, DGT concentrations are expected to approximate DET concentrations. Using the mean C_{DGT} and DET concentrations across the depth profiles (n = 15), it is clear that many $R_{c,72hr}$ values are below even the threshold for diffusive only supply ($R_{c,72hr}$ = 0.07) in these sediments (Figure 4). This may be because of spatial and temporal differences in solute supply / concentrations in the sediments or speciation effects on the DGT measurement. Sediments are famously heterogeneous and small-scale variability can confound the direct comparison of DET and DGT measurements carried out in different parts of the sediment (Huang et al., 2019). Interpretation of $R_{c,72h}$ values across the depth profile could also be confounded by localized changes in pore water chemistry that could

conceivably affect the lability of U to DGT at different depths. Our measurements did not provide evidence for such changes in these sediments.

The $R_{c,72h}$ values in the surface water were also low and these cannot be explained by spatial heterogeneity. Moreover, the supply of solutes to the DGT are not expected to be limited in flowing surface water to the same extent as in sediments. It is important to recognize that C_{DGT} represents a time-integrated mean concentration across the 72 hour measurement period, whereas the DET concentration only reflects conditions within the ~2 hours preceding the end of the deployment, hence temporal differences in U supply from the sediment through variation in hyporheic water flow and exchange may also be important here. Although the data presented here do not allow for complementary analysis of temporal changes in hyporheic flow conditions or solute supply to sediment pore waters and the overlying river water, evidence of temporal (< 24 hour) shifts in sediment pore water U concentrations was found at this study site (Figure S2).

Focusing on solute supply to the DGT in the surface water and sediment deployments, we can examine more closely if the U flux demanded by the DGT was greater than solute supply by deploying DGT probes with different material diffusion layer thicknesses. In both surface water and sediment deployments, a linear relationship between U accumulation and the material diffusion layer thickness is evident for probes with layer thicknesses of 0.092 to 0.208 cm (Figure 5), indicating sufficient solute supply to satisfy demand from the DGT probes at 10 cm depth at WR17-6. However, in both the sediment and surface water deployments, probes utilizing the 0.054 cm layer thickness deviated from linearity. Evidently, for deployments using the thinnest diffusion layer, which demands a higher flux from sediments to the probe, the local supply of solute was exhausted (Zhang et al., 1995). As the DGT field deployments in this study used a diffusion layer thickness of 0.092 cm, we can assume that solute supply to the DGT probe was not limiting

accumulation, and spatial and temporal heterogeneity is a possible factor behind the low $R_{c,\ 72hr}$ values at this location (Figure 4). However, the reduction in the mass accumulated by the probes with the thinnest diffusion layer in the surface water deployments (Figure 5b) indicates that competition for binding sites on the DGT may be important here, as the thinnest diffusion layer would also allow the greatest fluxes of other solute that can outcompete the U for the resin binding sites, thus reducing the total U uptake. It is therefore possible that U species that are inert, partially labile or not bound by DGT resin gel play an important role.

To establish the dominant U species in solution, PHREEQC modelling of aqueous U(VI) was conducted. The analysis indicates U speciation was dominated (>98%) by ternary uranyl (Ca or Mg) carbonate complexes in all sediment pore water at 15 cm depth and in surface water, with the uncharged $Ca_2UO_2(CO_3)_3$ complex accounting for 66-80% of all aqueous U species (Table S2). This is important as uncharged U complexes are unlikely to bind to the DGT resin but will be measured by DET, thus contributing to the low $R_{c,\ 72hr}$ values observed. Furthermore, only a small fraction of the total U concentration is present as the dicarbonato U species ($UO_2(CO_3)_2^{2-}$), which has previously been found to best predict U bioavailability to a model invertebrate (Croteau et al., 2016).

Several studies also point to ion competition as a potential explanation for low U accumulation in DGT probes. In laboratory experiments, and in the absence of competing ligands, Ca (< 250 mg L^{-1}) has been shown to aid U uptake on the DGT Metsorb™ gel by forming labile calcium uranyl species (Turner et al., 2012). However, U uptake was reduced at Ca concentrations > 250 mg L^{-1}. Sediment pore water samples (15 cm depth) at the Riverton site had Ca concentrations 331 to 861 mg L^{-1} and surface water averaged 72 mg L^{-1} (Naftz et al., 2019). Yet, DGT probes deployed in both environments had low $R_{c,\ 72hr}$ values. Other potential U complexants such as SO_4 were

reported to have no interference effects on U uptake (Turner et al., 2012) however the test range in that study (0.02 to 200 mg L^{-1}) was below the range of SO_4 concentrations in Riverton surface and sediment pore water (15 cm depth) (204 to 6740 mg L^{-1}) (Naftz et al., 2019). Turner et al. (2012) report U uptake was negatively affected by increasing HCO_3 (0.1 to 500 mg L^{-1}) and PO_4 (0.005 to 5 mg L^{-1}) concentration. Bicarbonate concentrations were elevated in the Riverton sediment pore waters at 15 cm depth (423 to 755 mg L^{-1}) and surface water (179 mg L^{-1}) (Naftz et al., 2019). Drozdzak et al. (2016) reported decreased U uptake on the DGT PIWBA resin in the presence of high Ca and SO_4 concentrations. Although these previous studies were not conducted under the same field conditions as the Little Wind River, they do provide evidence that major ion concentrations (Ca, SO_4, HCO_3) in the sediment pore water and surface water were at high enough concentrations to slow U accumulation in the DGT probes due to competition effects.

A final factor potentially limiting U accumulation in the DGT resins was the presence of U-dissolved organic matter (DOM) complexes. Dissolved organic matter is well known to limit the toxicity of certain metals (Paller et al., 2019). This effect is represented in DGT by the small diffusion co-efficient and partial lability of many DOM-metal complexes (Davison and Zhang, 2012). Whilst U-DOM species have been shown to limit U bioavailability to some freshwater invertebrate species (Croteau et al., 2016), the effect of U complexation by DOM in the present study, which ranges from 5 mg C L^{-1} in surface water to > 30 mg C L^{-1} in the contaminated groundwater at 1 m depth (Naftz et al., 2019), could not be considered in the PHREEQC speciation modelling. This is because the binding constants for U complexation by the DOM at this site are unknown. Therefore, the extent of U complexation by DOM in the Little Wind River groundwater and surface water system could not be examined.

3.3 Implications for monitoring U in groundwater-surface water systems

A growing number of studies worldwide report elevated concentrations of U in groundwater and drinking water (Banning et al., 2017; Coyte et al., 2018; Nolan and Weber, 2015; Nriagu et al., 2012). With many global regions demonstrating a climate shift towards aridity (Garreaud et al., 2020; Kogan and Guo, 2015), groundwater will become an increasingly more important source of water for humans (Dalin et al., 2017) and have a greater influence on surface water quality (Lansdown et al., 2015). It is therefore critical to develop and test methods to establish: (1) the degree of connectivity between groundwater and surface water systems, and (2) the potential water quality and ecological effects of contaminated groundwater on surface water systems.

In this study, streambed temperature surveys combined with DET and DGT groundwater (shallow sediment) and surface water measurements of solute chemistry have been demonstrated as a reliable method of establishing the location of diffuse (U-rich) groundwater efflux to surface water, and the magnitude of the effect on surface water and ground water quality. Sediment pore water contamination was substantial when mean plume U concentrations are compared to background concentrations and drinking water standards. However, a decrease in U pore water concentrations occurred above approximately 6 cm depth, hypothesized to be a combination of shallow groundwater mixing with lower concentration surface water, and precipitation and / or sorption of U solutes to the sediment. These processes could have a substantial bearing on ecosystem health as the hyporheic zone (defined here as the zone of surface water and ground water mixing) has been widely documented as an important habitat and refugium for aquatic organisms (Krause et al., 2011; Stubbington et al., 2011). Furthermore, although the groundwater plume appeared to increase U concentrations in the receiving surface water environment, surface water U concentrations remained below the drinking water standard. Therefore, surface water

quality effects from U-rich groundwater plumes may be negligible if the hydrological and geochemical environment in the riverbed sediments promotes attenuation through geochemical reaction, and if the dilution capacity of the surface water system is sufficient to maintain U concentrations below environmental quality standards.

The findings of this study indicate aqueous U in the Little Wind River had limited bioavailability. This is inferred from low accumulation of U in the DGT sediment pore water and surface water probes and the dominance of the uncharged $Ca_2UO_2(CO_3)_3$ aqueous complex determined by speciation modelling. This is consistent with low concentrations of U measured in aquatic invertebrates sampled at this site (Naftz et al., 2019). Considering the dominance of uncharged $Ca_2UO_2(CO_3)_3$ at the Riverton site, the high concentrations of solutes known to compete with U for DGT binding sites, and the inferred low U bioavailability from DGT investigations, analysis of groundwater and surface water chemistry at other UMTRCA sites allows us to offer some initial insights on the potential bioavailability of U at these sites. Figure 6 illustrates a comparison of groundwater and surface water chemistry at seven UMTRCA sites across the western U.S.A (data obtained from GEMS database; U.S. Department of Energy Legacy Management, 2020). Similar to Riverton, water chemistry is broadly characterized as calcium, bicarbonate and sulfate-type, with high total dissolved solids (240 12000 mg L^{-1}) and high concentrations of ions (Ca, SO_4, Na, HCO_3) known to compete with U for biological uptake sites in DGT probes and model organisms. Although we have not performed PHREEQC speciation analyses of these waters, or deployed DGT probes, it is reasonable at this stage to hypothesize that U bioavailability might be limited at these sites through complexation and / or competition effects. However, further investigations at the highlighted UMTRCA sites would be needed in order to verify this hypothesis.

4. Conclusions

Growing concerns over U contamination of groundwater, combined with increasing relevance of groundwater resources for drinking water and riverine ecosystems, have highlighted the need to understand the environmental risk of U in groundwater-surface water systems. To this end, this study has presented a methodological framework to establish the transport of U from groundwater to surface water and its potential ecological effects. We applied this methodology in the Little Wind River where U-rich groundwater is interacting with surface water downgradient from the former Riverton U mill and tailings disposal site. This site is typical of many former mill sites in the western U.S.A. now under the management of the DOE. Streambed temperature mapping was initially used to identify a broad zone of groundwater discharge to the river. Diffusive equilibrium in thin-film (DET) probes were then used to map vertical and longitudinal patterns in sediment pore water U and Sr concentrations. This further constrained the zone of groundwater discharge, and demonstrated decreases in U concentrations in the shallow sediment pore waters through groundwater-surface water interaction processes. An increase in river U concentrations was observed in the area of groundwater discharge; however, concentrations did not exceed environmental guidelines. This is the first time that contaminated groundwater at UMTRCA sites has been shown to affect surface waters and emphasizes the importance of a carefully designed and targeted sampling strategy to establish the effect of groundwater plume discharge on surface waters. Low accumulation of U in diffusive gradients in thin film (DGT) samplers, and the dominance of the uncharged $Ca_2UO_2(CO_3)_3$ complex, indicates limited bioavailability of this element in this river system. Further, we hypothesize low U bioavailability at other former mill sites in the western U.S.A. due to similar groundwater and surface water chemistry. However, the

extent of U complexation by DOM was not explored in this study and further investigation of the role of DOM in aqueous U speciation and DGT measurements is warranted. Application of the methodological framework used in this study at other DOE and worldwide sites with legacy groundwater issues may be highly beneficial to establish the extent of surface water and ecosystem contamination in groundwater-surface water systems.

CRediT authorship contribution statement

Patrick Byrne: Conceptualization, Methodology, Investigation, Formal analysis, Visualization, Writing – original draft, Writing – review and editing. **Christopher C. Fuller**: Conceptualization, Methodology, Formal analysis – geochemical modelling, Writing – review and editing. **David L. Naftz**: Conceptualization, Methodology, Writing – review and editing, Supervision. **Robert L. Runkel**: Conceptualization, Methodology, Formal analysis, Writing – review and editing. **Niklas J. Lehto**: Methodology, Formal analysis – DIFS modelling, Writing – review and editing; **William L. Dam**: Writing – review and editing.

Declaration of competing interest

The authors declare that they have no known competing financial interests or personal relationships that could have appeared to influence the work reported in this paper.

Acknowledgements

This research was co-funded by the U.S. Department of Energy, Office of Legacy Management's Applied Science and Technology Program, and the U.S. Geological Survey Toxic Substances Hydrology Program. We thank U.S. Geological Survey staff at the Riverton field office

for helping with and facilitating field and laboratory investigations. Any use of trade, firm, or product names is for descriptive purposes only and does not imply endorsement by the U.S. Government.

Figure and table captions

Figure 1. Study area on the Little Wind River, Riverton, Wyoming, U.S.A., showing all DET and DGT sediment and surface water sampling sites. Top left inset shows location of selected UMTRCA sites in the USA. Bottom right inset shows the location of the former Riverton Processing Site and the approximate boundary and flow direction of the U-rich groundwater plume.

Figure 2. (a) Streambed temperature profile along the left bank of the Little Wind River from August 2017. Sediment pore water uranium (b) and strontium (c) concentrations obtained from DET measurements along the left bank of the Little Wind River.

Figure 3. Comparison of surface water uranium concentrations from upstream to downstream from the location of groundwater entry to the Little Wind River, showing (a) grab samples, (b) DET measurements, and (c) DGT measurements. Error bars in Figure 3a are the standard deviation of three samples collected at the left side, center, and right side of a transect along the river. Error bars in Figures 3b and 3c are the standard deviation of triplicate measurements from the left bank of the river only. Riv-U/S = sample site upstream from the plume. Riv-Mid = sample site at approximately the location of the plume. Riv-D/S = sample site downstream from the plume.

Figure 4. Accumulation of uranium in sediment (WR17) and surface water (Riv) DGT probes represented as $R_{c,\ 72hr}$, the ratio of C_{DGT} from a 72 hour deployment to the bulk pore water solute

concentrations from DET measurements. $R_{c,\ 72hr} > 0.8$ = sustained case; $0.07 < R_{c,\ 72hr} > 0.8$ = partially sustained case; $R_{c,\ 72hr} < 0.07$ = diffusive case. Error bars are the standard deviation of 15 measurements for sediment samplers and 3 measurements for surface water samplers. Vertical solid lines represent the approximate upstream and downstream boundaries of the groundwater plume entry to the Little Wind River. Samples are shown from upstream (left) to downstream (right).

Figure 5. Measured mass per unit area of uranium plotted against the reciprocal of the material diffusion layer thickness (Δg) in the DGT probes deployed in (a) shallow sediments (10 cm depth) and (b) surface waters for 72 hrs. Error bars are the standard deviation of triplicate measurements.

Figure 6. Piper plot showing the major ion chemistry of ground and surface water at selected UMTRCA sites, including the former Riverton Processing site. Data represent the most recent sample available from a single measurement site on the GEMS database [U.S. Department of Energy Legacy Management, 2020]. GW = groundwater sample. SW = surface water sample.

Table 1. Summary of uranium concentrations in $\mu g\ L^{-1}$ from DET and DGT deployments and surface water grab samples in the Little Wind River. Data for surface water (SW) grab samples are concentrations at the start and end of surface water DET and DGT deployments. Data for sediment pore water (PW) samples are mean, minimum, and maximum concentrations.

References

Abdelouas A. Uranium Mill Tailings: Geochemistry, Mineralogy, and Environmental Impact. Elements 2006; 2: 335-341.

Amato ED, Simpson SL, Jarolimek CV, Jolley DF. Diffusive gradients in thin films technique provide robust prediction of metal bioavailability and toxicity in estuarine sediments. Environ Sci Technol 2014; 48: 4485-94.

592 Banning A, Pawletko N, Röder J, Kübeck C, Wisotzky F. Ex situ groundwater treatment triggering
593 the mobilization of geogenic uranium from aquifer sediments. Science of The Total
594 Environment 2017; 587-588: 371-380.
595 Bennett WW, Arsic M, Panther JG, Welsh DT, Teasdale PR. Binding Layer Properties. In:
596 Davison W, editor. Diffusive Gradients in Thin-Films for Environmental Measurements.
597 Cambridge University Press, Cambridge, 2016, pp. 66-92.
598 Bjørklund G, Semenova Y, Pivina L, Dadar M, Rahman MM, Aaseth J, et al. Uranium in drinking
599 water: a public health threat. Archives of Toxicology 2020.
600 Bone SE, Cahill MR, Jones ME, Fendorf S, Davis J, Williams KH, et al. Oxidative Uranium
601 Release from Anoxic Sediments under Diffusion-Limited Conditions. Environ Sci Technol
602 2017a; 51: 11039-11047.
603 Bone SE, Dynes JJ, Cliff J, Bargar JR. Uranium(IV) adsorption by natural organic matter in anoxic
604 sediments. Proc Natl Acad Sci U S A 2017b; 114: 711-716.
605 Byrne P, Binley A, Heathwaite AL, Ullah S, Heppell CM, Lansdown K, et al. Control of river
606 stage on the reactive chemistry of the hyporheic zone. Hydrological Processes 2014; 28:
607 4766-4779.
608 Byrne P, Zhang H, Ullah S, Binley A, Heathwaite AL, Heppell CM, et al. Diffusive equilibrium
609 in thin films provides evidence of suppression of hyporheic exchange and large-scale
610 nitrate transformation in a groundwater-fed river. Hydrological Processes 2015; 29: 1385-
611 1396.
612 Cánovas CR, Basallote MD, Borrego P, Millán-Becerro R, Pérez-López R. Metal partitioning and
613 speciation in a mining-impacted estuary by traditional and passive sampling methods.
614 Science of The Total Environment 2020; 722: 137905.
615 Conant B. Delineating and quantifying ground water discharge zones using streambed
616 temperatures. Ground Water 2004; 42: 243-257.
617 Coyte RM, Jain RC, Srivastava SK, Sharma KC, Khalil A, Ma L, et al. Large-Scale Uranium
618 Contamination of Groundwater Resources in India. Environmental Science & Technology
619 Letters 2018; 5: 341-347.
620 Croteau MN, Fuller CC, Cain DJ, Campbell KM, Aiken G. Biogeochemical Controls of Uranium
621 Bioavailability from the Dissolved Phase in Natural Freshwaters. Environ Sci Technol
622 2016; 50: 8120-7.
623 Dalin C, Wada Y, Kastner T, Puma MJ. Groundwater depletion embedded in international food
624 trade. Nature 2017; 543: 700-704.
625 Dam WL, Campbell S, Johnson RH, Looney BB, Denham ME, Eddy-Dilek CA, et al. Refining
626 the site conceptual model at a former uranium mill site in Riverton, Wyoming, USA.
627 Environmental Earth Sciences 2015; 74: 7255-7265.
628 Davison W, Zhang H. Progress in understanding the use of diffusive gradients in thin films (DGT)
629 – back to basics. Environmental Chemistry 2012; 9: 1-13.
630 Davison W, Zhang H. Diffusive gradients in thin-films for environmental measurements.
631 Cambridge: Cambridge University Press, 2016.
632 DeGryse F, Smolders E. DGT and Bioavailability. In: Davison W, editor. Diffuse Gradients in
633 Thin-Films for Environmental Measurements. Cambridge University Press, Cambridge,
634 2016.
635 Dong W, Brooks SC. Determination of the Formation Constants of Ternary Complexes of Uranyl
636 and Carbonate with Alkaline Earth Metals (Mg2+, Ca2+, Sr2+, and Ba2+) Using Anion
637 Exchange Method. Environmental Science & Technology 2006; 40: 4689-4695.

638 Dong W, Brooks SC. Formation of Aqueous MgUO2(CO3)32− Complex and Uranium Anion
639 Exchange Mechanism onto an Exchange Resin. Environmental Science & Technology
640 2008; 42: 1979-1983.
641 Drozdzak J, Leermakers M, Gao Y, Phrommavanh V, Descostes M. Novel speciation method
642 based on Diffusive Gradients in Thin Films for in situ measurement of uranium in the
643 vicinity of the former uranium mining sites. Environ Pollut 2016; 214: 114-123.
644 Dunk RM, Mills RA, Jenkins WJ. A reevaluation of the oceanic uranium budget for the Holocene.
645 Chemical Geology 2002; 190: 45-67.
646 Fuller CC, Harvey JW. Reactive uptake of trace metals in the hyporheic zone of a mining-
647 contaminated stream, Pinal Creek, Arizona. Environmental Science & Technology 2000;
648 34: 1150-1155.
649 Garreaud RD, Boisier JP, Rondanelli R, Montecinos A, Sepulveda HH, Veloso-Aguila D. The
650 Central Chile Mega Drought (2010-2018): A climate dynamics perspective. International
651 Journal of Climatology 2020; 40: 421-439.
652 Gregusova M, Docekal B. High resolution characterization of uranium in sediments by DGT and
653 DET techniques ACA-S-12-2197. Anal Chim Acta 2013; 763: 50-6.
654 Guillaumont R, Fanghangel T, Fuger J, Grenthe I, Neck V, Palmer DA, et al. Update on the
655 chemical thermodynamics of uranium, neptunium, plutonium, americium and technetium.
656 Amsterdam: Elsevier, 2003.
657 Guo H, Jia Y, Wanty RB, Jiang Y, Zhao W, Xiu W, et al. Contrasting distributions of groundwater
658 arsenic and uranium in the western Hetao basin, Inner Mongolia: Implication for origins
659 and fate controls. Science of The Total Environment 2016; 541: 1172-1190.
660 Gupta C, Singh H. Uranium Resource Processing. Secondary Resources.: Springer, 2003.
661 Harper MP, Davison W, Tych W. DIFS—a modelling and simulation tool for DGT induced trace
662 metal remobilisation in sediments and soils. Environmental Modelling & Software 2000;
663 15: 55-66.
664 Harper MP, Davison W, Zhang H, Tych W. Kinetics of metal exchange between solids and
665 solutions in sediments and soils interpreted from DGT measured fluxes. Geochimica et
666 Cosmochimica Acta 1998; 62: 2757-2770.
667 Huang J, Franklin H, Teasdale PR, Burford MA, Kankanamge NR, Bennett WW, et al.
668 Comparison of DET, DGT and conventional porewater extractions for determining nutrient
669 profiles and cycling in stream sediments. Environmental Science: Processes & Impacts
670 2019; 21: 2128-2140.
671 Hutchins CM, Panther JG, Teasdale PR, Wang F, Stewart RR, Bennett WW, et al. Evaluation of
672 a titanium dioxide-based DGT technique for measuring inorganic uranium species in fresh
673 and marine waters. Talanta 2012; 97: 550-6.
674 Kogan F, Guo W. 2006-2015 mega-drought in the western USA and its monitoring from space
675 data. Geomatics Natural Hazards & Risk 2015; 6: 651-668.
676 Krause S, Hannah DM, Fleckenstein JH, Heppell CM, Kaeser D, Pickup R, et al. Inter-disciplinary
677 perspectives on processes in the hyporheic zone. Ecohydrology 2011; 4: 481-499.
678 Lansdown K, Heppell CM, Trimmer M, Binley A, Heathwaite AL, Byrne P, et al. The interplay
679 between transport and reaction rates as controls on nitrate attenuation in permeable,
680 streambed sediments. Journal of Geophysical Research-Biogeosciences 2015; 120: 1093-
681 1109.

682 Lehto NJ. Principles and application in soils and sediments. In: Davison W, Zhang H, editors.
683 Diffusive gradients in thin-films for environmental measurements. Cambridge University
684 Press, Cambridge, 2016.
685 Ma X, Li C, Yang L, Ding S, Zhang M, Zhang Y, et al. Evaluating the mobility and labile of As
686 and Sb using diffusive gradients in thin-films (DGT) in the sediments of Nansi Lake,
687 China. Science of The Total Environment 2020; 713: 136569.
688 Menezes-Blackburn D, Sun J, Lehto NJ, Zhang H, Stutter M, Giles CD, et al. Simultaneous
689 Quantification of Soil Phosphorus Labile Pool and Desorption Kinetics Using DGTs and
690 3D-DIFS. Environmental Science & Technology 2019; 53: 6718-6728.
691 Merritt SJ. The extractive metallurgy of uranium. Golden: Johnson Publishing Co, 1971.
692 Naftz DL, Fuller CC, Runkel RL, Brigss MA, Solder JE, Cain DJ, et al. Hydrologic,
693 biogeochemical, and radon data collected within and adjacent to the Little Wind River near
694 Riverton, Wyoming. U.S. Geological Survey data release,
695 https://doi.org/10.5066/F7BR8QX4., 2019.
696 Narasimhan TN, White AF, Tokunaga T. Groundwater contamination from an inactive uranium
697 mill tailings pile: 2. Application of a dynamic mixing model. Water Resources Research
698 1986; 22: 1820-1834.
699 Nolan J, Weber KA. Natural Uranium Contamination in Major U.S. Aquifers Linked to Nitrate.
700 Environmental Science & Technology Letters 2015; 2: 215-220.
701 Nriagu J, Nam D-H, Ayanwola TA, Dinh H, Erdenechimeg E, Ochir C, et al. High levels of
702 uranium in groundwater of Ulaanbaatar, Mongolia. Science of The Total Environment
703 2012; 414: 722-726.
704 Paller MH, Harmon SM, Knox AS, Kuhne WW, Halverson NV. Assessing effects of dissolved
705 organic carbon and water hardness on metal toxicity to Ceriodaphnia dubia using diffusive
706 gradients in thin films (DGT). Science of The Total Environment 2019; 697: 134107.
707 Parker R, Bolam T, Barry J, Mason C, Kroger S, Warford L, et al. The application of Diffusive
708 Gradients in Thin Films (DGT) for improved understanding of metal behaviour at marine
709 disposal sites. Science of the Total Environment 2017; 575: 1074-1086.
710 Parkhurst DL, Appelo CAJ. Description of input and examples for PHREEQC version 3—A
711 computer program for speciation, batch-reaction, one-dimensional transport, and inverse
712 geochemical calculations. Vol U.S. Geological Survey Techniques and Methods, book 6,
713 chapter A43, 2013.
714 Petelet-Giraud E, Négrel P, Casanova J. Tracing surface water mixing and groundwater inputs
715 using chemical and isotope fingerprints (δ18O-δ2H, 87Sr/86Sr) at basin scale: The Loire
716 River (France). Applied Geochemistry 2018; 97: 279-290.
717 Pinney SM, Freyberg RW, Levine GE, Brannen DE, Mark LS, Nasuta JM, et al. Health effects in
718 community residents near a uranium plant at Fernald, Ohio, USA. International Journal of
719 Occupational Medicine and Environmental Health 2003; 16: 139-153.
720 Ranalli AJ, Naftz DL. Assessment of the quality of groundwater and the Little Wind River in the
721 area of a former uranium processing facility on the Wind River Reservation, Wyoming,
722 1987 through 2010, 2014, pp. 104.
723 Shafer D, Bush R, Dam WL, Pauling T. The future is now: experience with remediating and
724 managing groundwater contamination at uranium mill tailing sites. Waste Management
725 Conference, Phoenix, Arizona, 2014.

Stockdale A, Davison W, Zhang H. Micro-scale biogeochemical heterogeneity in sediments: A review of available technology and observed evidence. Earth-Science Reviews 2009; 92: 81-97.
Stubbington R, Wood PJ, Reid I. Spatial variability in the hyporheic zone refugium of temporary streams. Aquatic Sciences 2011; 73: 499-511.
Terry N, Briggs MA. Geophysical data collected within and adjacent to the Little Wind River near Riverton, Wyoming. U.S. Geological Survey data release, https://doi.org/10.5066/P9J9VJBR, 2019.
Turner GSC, Mills GA, Bowes MJ, Burnett JL, Amos S, Fones GR. Evaluation of DGT as a long-term water quality monitoring tool in natural waters; uranium as a case study. Environmental Science-Processes & Impacts 2014; 16: 393-403.
Turner GSC, Mills GA, Teasdale PR, Burnett JL, Amos S, Fones GR. Evaluation of DGT techniques for measuring inorganic uranium species in natural waters: Interferences, deployment time and speciation. Analytica Chimica Acta 2012; 739: 37-46.
U.S. Department of Energy. Baseline risk assessment of ground water contamination at the uranium mill tailings site near Riverton, Wyoming, 1995, pp. 166.
U.S. Department of Energy. Final Site Observational Work Plan for the UMTRA Project Site at Riverton, Wyoming, 1998.
U.S. Department of Energy. Verification monitoring report, Riverton, Wyoming, 2009.
U.S. Department of Energy. UMTRA Title I and II Fact Sheet. U.S. Department of Energy, Grand Junction, 2020.
U.S. Department of Energy Legacy Management. Geospatial Environmental Mapping System. U.S. Department of Energy Legacy Management, 2020.
U.S. Environmental Protection Agency. National Primary Drinking Water Regulations; Radionuclides; Final Rule. U.S. Environmental Protection Agency, 2000.
U.S. GAO (U.S. Government Accountability Office). Environmental Liabilities. DOE needs to better plan for post-cleanup challenges facing sites, 2020.
Ullah S, Zhang H, Heathwaite AL, Binley A, Lansdown K, Heppell K, et al. In situ measurement of redox sensitive solutes at high spatial resolution in a riverbed using Diffusive Equilibrium in Thin Films (DET). Ecological Engineering 2012; 49: 18-26.
White AF, Delany JM, Narasimhan TN, Smith A. Groundwater contamination from an inactive uranium mill tailings pile: 1. Application of a chemical mixing model. Water Resources Research 1984; 20: 1743-1752.
Windom H, Smith R, Niencheski F, Alexander C. Uranium in rivers and estuaries of globally diverse, smaller watersheds. Marine Chemistry 2000; 68: 307-321.
World Health Organization (WHO). Uranium in Drinking-water. Background document for development of WHO Guidelines for Drinking-water Quality. World Health Organization, Geneva, Switzerland, 2012.
World Nuclear Association. The Nuclear Fuel Report: Global scenarios for demand and supply availability 2019-2040. World Nuclear Association, 2019.
Zachara JM, Long PE, Bargar J, Davis JA, Fox P, Fredrickson JK, et al. Persistence of uranium groundwater plumes: Contrasting mechanisms at two DOE sites in the groundwater–river interaction zone. Journal of Contaminant Hydrology 2013; 147: 45-72.
Zhang H, Davison W, Miller S, Tych W. In-Situ High-Resolution Measurements of Fluxes of Ni, Cu, Fe, and Mn and Concentrations of Zn and Cd in Porewaters by DGT. Geochimica Et Cosmochimica Acta 1995; 59: 4181-4192.

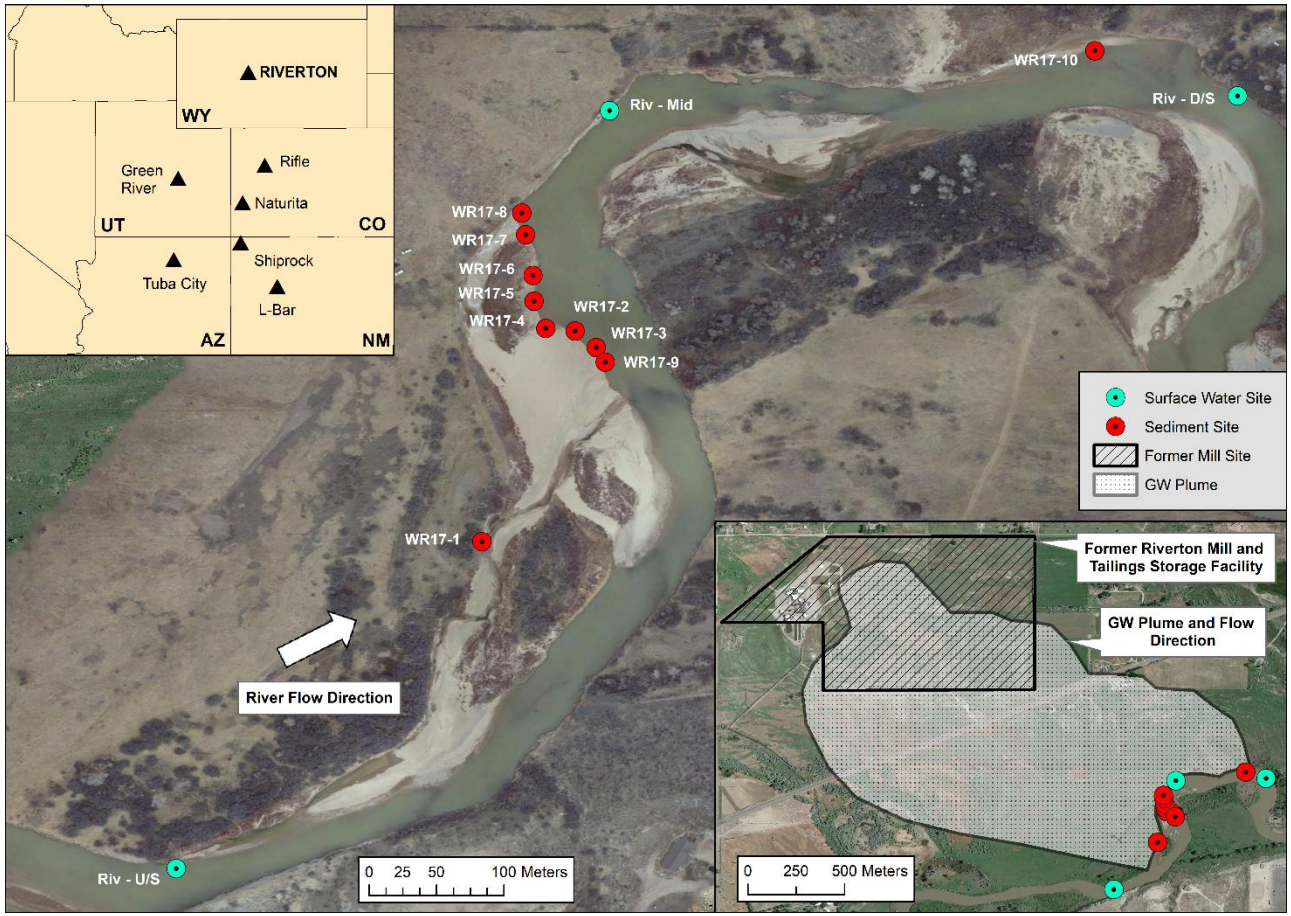

773

774 Figure 1. Study area on the Little Wind River, Riverton, Wyoming, U.S.A., showing all DET and DGT sediment and surface water

775 sampling sites. Top left inset shows location of selected UMTRCA sites in the USA. Bottom right inset shows the location of the former

776 Riverton Processing Site and the approximate boundary and flow direction of the U-rich groundwater plume.

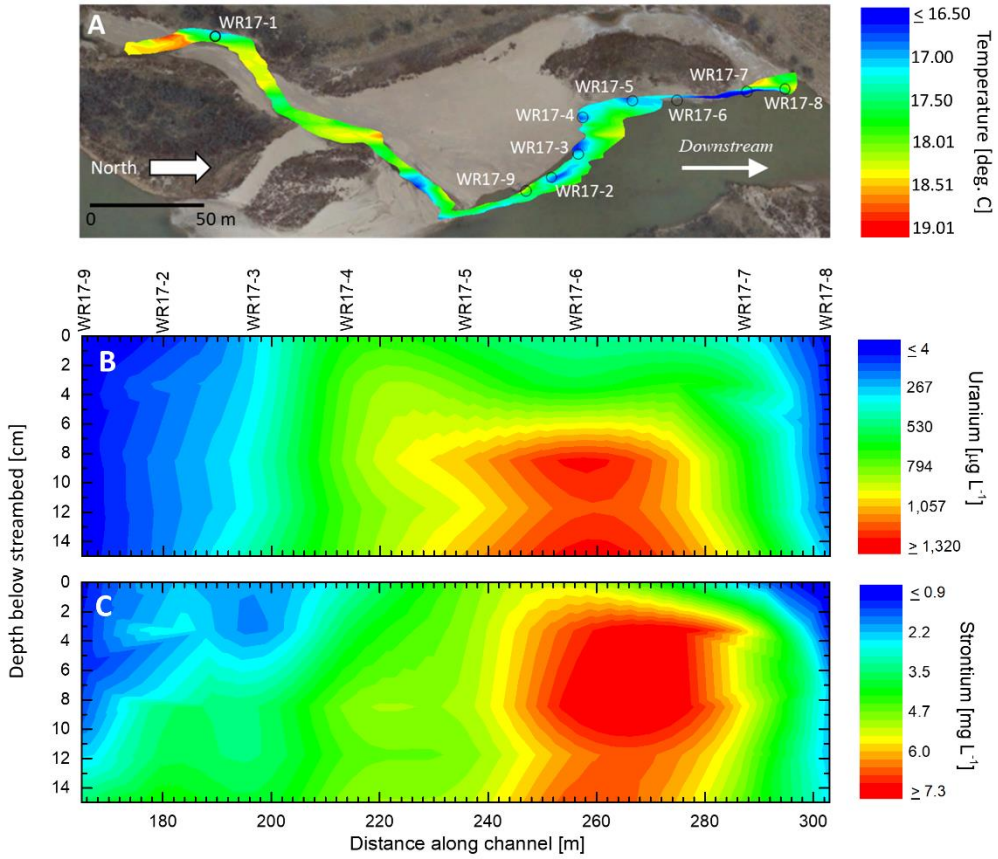

777

778 Figure 2. (a) Streambed temperature profile along the left bank of the Little Wind River from August 2017. Sediment pore water uranium

779 (b) and strontium (c) concentrations obtained from DET measurements along the left bank of the Little Wind River.

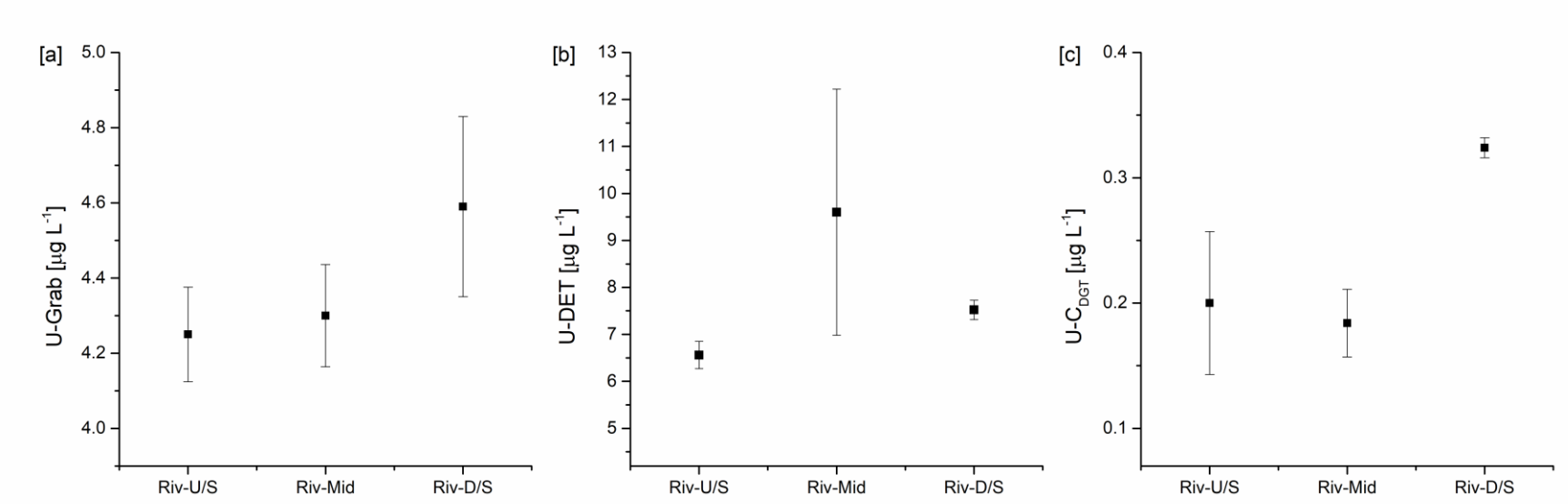

Figure 3. Comparison of surface water uranium concentrations from upstream to downstream from the location of groundwater entry to the Little Wind River, showing (a) grab samples, (b) DET measurements, and (c) DGT measurements. Error bars in Figure 3a are the standard deviation of three samples taken at the left side, centre, and right side of a transect along the river. Error bars in Figures 3b and 3c are the standard deviation of triplicate measurements from the left bank of the river only. Riv-U/S = sample site upstream of the plume. Riv-Mid = sample site at approximately the location of the plume. Riv-D/S = sample site downstream of the plume.

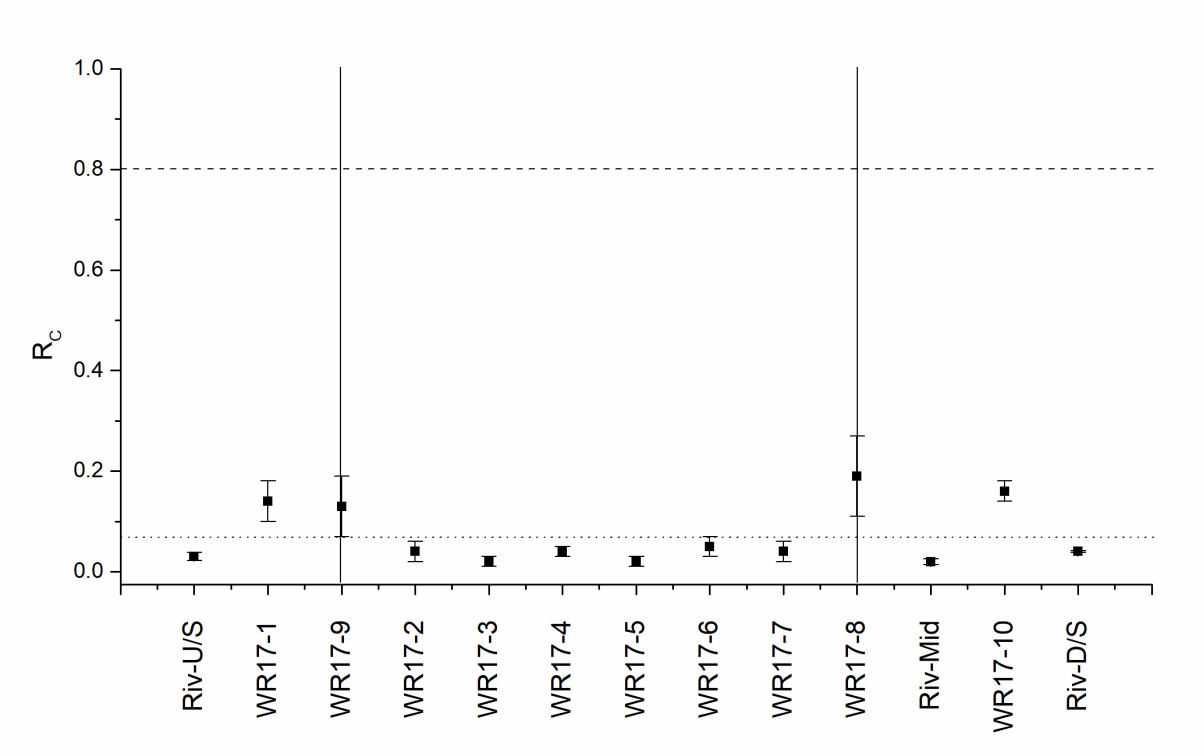

Figure 4. Accumulation of uranium in sediment (WR17) and surface water (Riv) DGT probes represented as $R_{c,\ 72hr}$, the ratio of C_{DGT} from a 72 hour deployment to the bulk pore water solute concentrations from DET measurements. $R_{c,\ 72hr} > 0.8$ = sustained case; $0.07 < R_{c,\ 72hr} > 0.8$ = partially sustained case; $R_{c,\ 72hr} < 0.07$ = diffusive case. Error bars are the standard deviation of 15 measurements for sediment samplers and 3 measurements for surface water samplers. Vertical solid lines represent the approximate upstream and downstream boundaries of the groundwater plume entry to the Little Wind River. Samples are shown from upstream (left) to downstream (right).

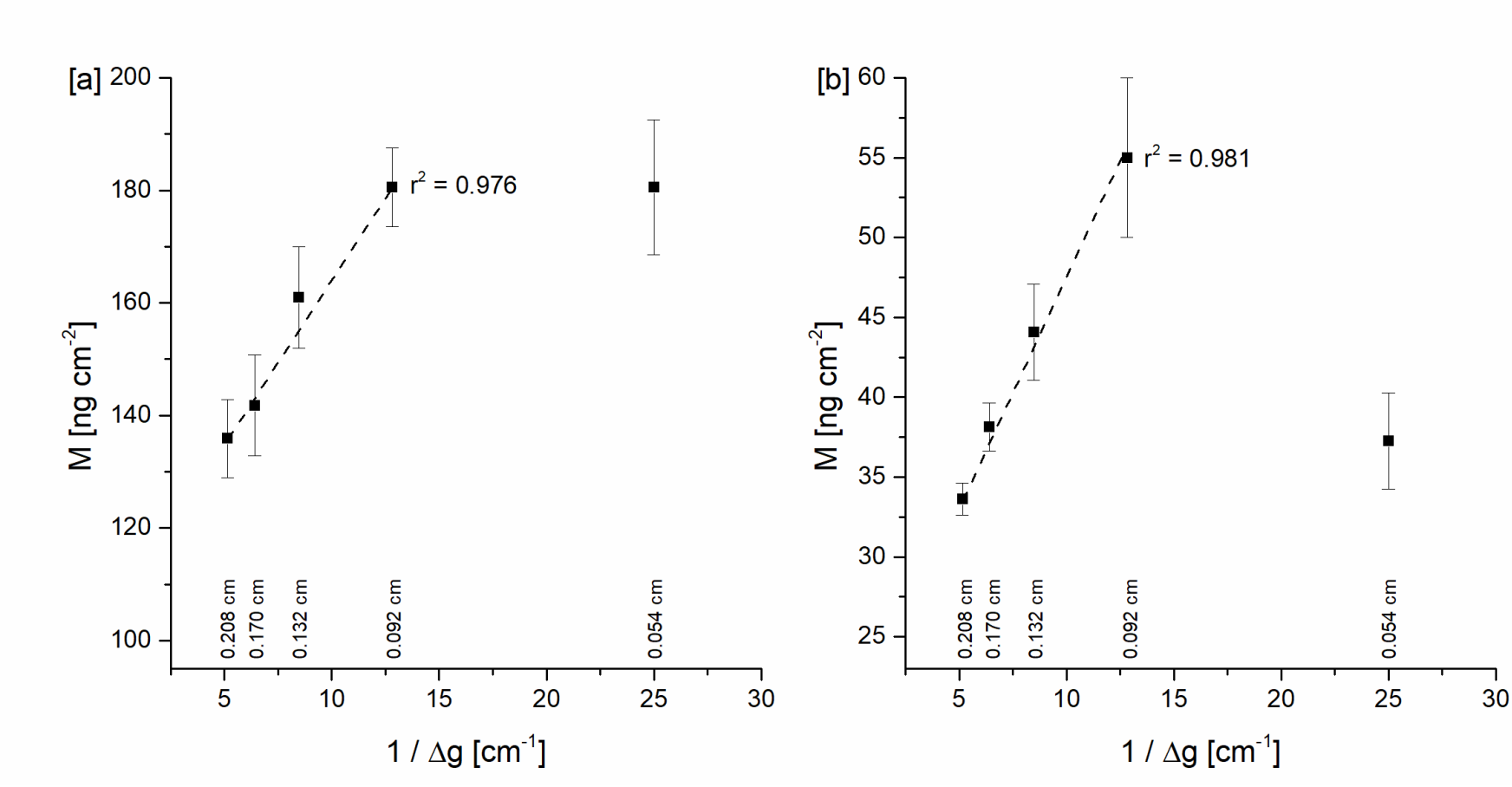

796

797 Figure 5. Measured mass per unit area of uranium plotted against the reciprocal of the material diffusion layer thickness (Δg) in the
798 DGT probes deployed in (a) shallow sediments (10 cm depth) and (b) surface waters for 72 hrs. Error bars are the standard deviation of
799 triplicate measurements.

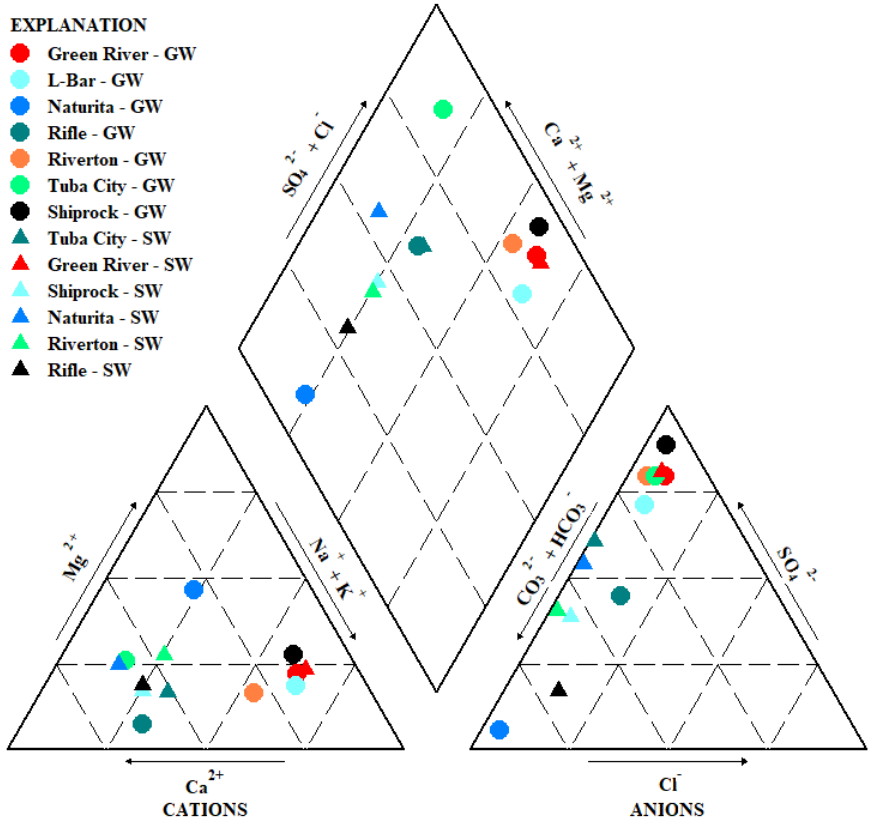

800

801 Figure 6. Piper plot showing the major ion chemistry of ground and surface water at selected UMTRCA sites, including the former

802 Riverton Processing site. Data represent the most recent sample available from a single measurement site on the GEMS database [U.S.

803 Department of Energy Legacy Management, 2020]. GW = groundwater sample. SW = surface water sample.

804

Table 1. Summary of uranium concentrations in μg L^{-1} from DET and DGT deployments and surface water grab samples in the Little Wind River. Data for surface water (SW) grab samples are concentrations at the start and end of surface water DET and DGT deployments. Data for sediment pore water (PW) samples are mean, minimum, and maximum concentrations.

	Riv-U/S	**Riv-Mid**	**Riv-D/S**		
Grab-SW (n = 2)	5.1 / 5.5	6.8 / 6.5	6.3 / 6.4		
DET-SW (n = 3)	6.7 (6.3 – 6.9)	9.6 (7.7 – 12.6)	7.5 (7.4 – 7.8)		
DGT-SW (n = 3)	0.2 (0.13 – 0.24)	0.18 (0.16 – 0.21)	0.32 (0.32 – 0.33)		
	WR17-1	**WR17-9**	**WR17-2**	**WR17-3**	**WR17-4**
DET-PW (n = 15)	21.5 (19.4 – 23.5)	4.8 (3.9 – 6.1)	179 (67 – 227)	351 (282 – 441)	794 (718 – 834)
DGT-PW (n = 15)	2.8 (1.9 – 4.4)	0.7 (0.3 – 1.6)	6.9 (2.3 – 14.5)	8.3 (6 – 13.5)	28.6 (15 – 47.4)
	WR17-5	**WR17-6**	**WR17-7**	**WR17-8**	**WR17-10**
DET-PW (n = 15)	903 (610 – 1049)	1010 (487 – 1321)	675 (449 – 861)	77 (31 – 148)	11.1 (8.9 – 14.3)
DGT-PW (n = 15)	19.6 (14.1 – 29.6)	56 (20.8 – 121.7)	21 (13.8 – 35.4)	11.5 (4.4 – 29)	1.8 (1.5 - 2.3)